



# “Post-It” Type Connected DNA Created with a Reversible Covalent Cross-Link\*\*

María Tomás-Gamasa, Sascha Serdjukow, Meng Su, Markus Müller, and Thomas Carell\*

Dedicated to Prof. José Barluenga on the occasion of his 75th birthday

**Abstract:** We report the development of a new heterobase that is held together through reversible bonding. The so-formed cross-link adds strong stabilization to the DNA duplex. Despite this, the cross-link opens and closes through reversible imine bonding. Moreover, even enzymatic incorporation of the cross-link is possible. The new principle can be used to stabilize DNA duplexes and nanostructures that otherwise require high salt concentrations, which may hinder biological applications.

DNA nanotechnology uses the superb self-organizing properties of oligonucleotides to assemble complex two- and three-dimensional objects.<sup>[1]</sup> Although controlling the complex assembly process was initially the focus of the research,<sup>[1f,2]</sup> we are now entering a phase where the construction of functional systems is desired.<sup>[2a,b,3]</sup> Examples include DNA nanostructures decorated with enzymes,<sup>[4]</sup> and nanocontainers which can release cargo in response to an outside stimulus.<sup>[5]</sup> In particular, the latter application requires the DNA-based nanostructures to be delivered to cells and living organisms. However, we encounter a fundamental problem with more complex DNA nanoobjects in living systems: DNA-based nanostructures require high salt concentrations for their formation and stability, and it is difficult to create stable structures under low salt concentrations, for example, inside cells. Thus far, DNA structures have been stabilized using disulfide linkages,<sup>[6]</sup> alkylating cross-links,<sup>[7]</sup> and unspecific UV-induced psoralene cross-links.<sup>[4a,8]</sup>

We report here the development of an enzymatically processable cross-link that provides DNA structures with high, but also reversible stability. The cross-linking “bases” (Figure 1 A) form a covalent connection over time that can, however, be reopened by heating. In this sense, the here

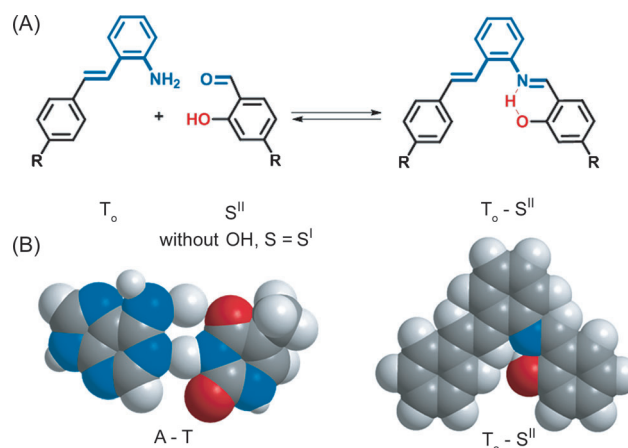


**Figure 1.** A) The aniline:(hydroxy)benzaldehyde cross-link ( $T_0:S^{II}$ ). B) Space-filling model of the  $T_0:S^{II}$  cross-link compared to the natural A:T base pair.

reported cross-link represents a “post-it”-type glue for DNA duplexes and, consequently, also for nanostructures in low salt concentrations.

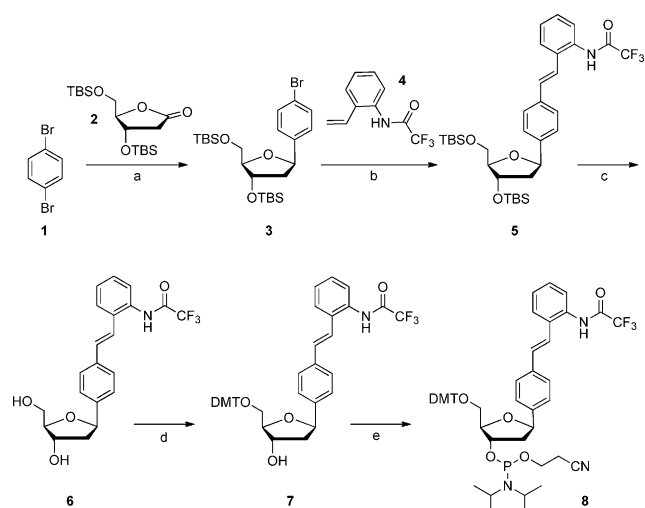
The cross-link  $T_0:S^{II}$  is created from an aromatic amine and a benzaldehyde base with a hydroxy group in the *ortho*-position ( $S^{II}$ ). During assembly, a reversible interstrand cross-link is formed between the nucleobases through an imine bond. The presence of the *ortho*-OH group is likely important to stabilize the structure, similar to the enzyme-bound pyridoxal phosphate.<sup>[9]</sup> A benzaldehyde base lacking the hydroxy group ( $S^I$ ) has been used to verify this hypothesis. It is interesting that imine bonding also occurs naturally between an adenine and a sugar of an opposite abasic site (A:AP).<sup>[10]</sup>

The synthesis of the amine nucleoside  $T_0$  was accomplished (Scheme 1) from 1,4-dibromobenzene (**1**), furo-lactone **2**, and the NH-protected vinylaniline **4**. The C-glycosidation was performed by addition of the monolithiated compound prepared from **1** to the TBS-protected 2'-deoxyribose furo-lactone **2**, followed by reduction to afford the  $\beta$ -arylfuranose derivative **3**.<sup>[11]</sup> Then, Heck coupling of *N*-trifluoroacetyled vinylaniline **4** (obtained in two steps from commercially available 2-bromoaniline) with the bromoarene **3** provided the *E*-alkene **5**. The trifluoroacetyl protecting group was found to be fully compatible with both the nucleoside preparation and the subsequent solid-phase DNA synthesis. Finally, compound **5** was transformed into the corresponding phosphoramidite building block for solid-

[\*] Dr. M. Tomás-Gamasa, M. Sc. S. Serdjukow, M. Sc. M. Su, Dr. M. Müller, Prof. Dr. T. Carell  
Department of Chemistry and Pharmacy  
Ludwig-Maximilians-Universität München  
Butenandtstrasse 5–13, 81377 München (Germany)  
E-mail: Thomas.Carell@lmu.de  
Homepage: <http://www.carellgroup.de>

[\*\*] M.T.-G. thanks the Alexander von Humboldt Foundation for a postdoctoral fellowship. We also owe gratitude to S. Schneider for the X-ray measurements. This work was supported by the Deutsche Forschungsgemeinschaft, SFB1032 (TP-A5), and SFB749 (TP-A4). Further support was obtained from the Cluster of Excellence Nanosystems Initiative Munich (NIM).

Supporting information for this article is available on the WWW under <http://dx.doi.org/10.1002/anie.201407854>.



**Scheme 1.** Synthesis of phosphoramidite **8** and the amine nucleobase **6**. a) 1. *n*BuLi (1.63 equiv), THF, 30 min,  $-78^{\circ}\text{C}$ ; 2. **2** (1.00 equiv), THF, 1 h,  $-78^{\circ}\text{C}$ ; 3.  $\text{Et}_3\text{SiH}$  (3.28 equiv),  $\text{BF}_3\cdot\text{OEt}_2$  (1.23 equiv),  $\text{CH}_2\text{Cl}_2$ , 2 h,  $-78^{\circ}\text{C}$ , 23%; b) **4** (1.25 equiv), 8 mol%  $\text{Pd}(\text{OAc})_2$ , 16 mol%  $\text{P}(\text{o-tol})_3$ ,  $\text{NEt}_3$ ,  $70^{\circ}\text{C}$ , 70%; c) HF-py,  $\text{NEt}_3$ , 6 h, 96%; d) DMT-Cl (1.1 equiv), pyridine, 3 h, 76%; e) CED-Cl (1.1 equiv),  $\text{NEt}_3$ , THF, 2 h, 92%. TBS = *tert*-butyldimethylsilyl, DMT = 4,4'-dimethoxytrityl, CED-Cl = 2-cyanoethyl *N,N*-diisopropylchlorophosphoramidite.

phase DNA synthesis. Cleavage of the *tert*-butylsilyl groups (compound **6**) and subsequent selective DMT-protection to afford nucleoside **7**, was followed by generation of the phosphoramidite **8**.

The aldehyde  $\text{S}^{\text{I}}$  was accessed by using a similar modular synthesis. It required the coupling of furulactone **2** with protected 4-bromobenzaldehyde followed by sequential deprotection and protection steps, and phosphoramidite formation (see p. 9 in the Supporting Information). The hydroxy aldehyde nucleobase  $\text{S}^{\text{II}}$  and its phosphoramidite were prepared according to published procedures.<sup>[12,18]</sup>

The  $\text{T}_0$ - and S-containing DNA oligonucleotides were then synthesized following standard solid-phase phosphoramidite protocols for oligonucleotide synthesis (Table 1). In the case of the  $\text{T}_0$  phosphoramidite, the capping step had to be avoided because of side reactions.<sup>[13]</sup> This was no limitation, because the coupling yields of  $\text{T}_0$  and all the subsequent bases were sufficiently high. Finally, treatment of the assembled DNA with aqueous  $\text{NH}_2\text{Me}/\text{NH}_3$  (1:1) at  $65^{\circ}\text{C}$  removed the

**Table 1:** Sequences of the oligonucleotides examined for  $T_m$  and CD experiments.

Duplex	Oligonucleotide sequences	$T_m$ [ $^{\circ}\text{C}$ ]
<b>D1a</b>	5'- CACATTA <sup>A</sup> TGTTGTA -3' 3'- GTGTAAT <sup>T</sup> ACAACAT -5'	48
<b>D1b</b>	5'- CACATTA <sup>C</sup> TGTTGTA -3' 3'- GTGTAAT <sup>A</sup> ACAACAT -5'	35
<b>D1c</b>	5'- CACATTAT <sup>T</sup> GTGTTGTA -3' 3'- GTGTAAT <sup>S</sup> ACAACAT -5'	38 <sup>[a]</sup> 42 <sup>[b]</sup>
<b>D1d</b>	5'- CACATTAT <sup>T</sup> GTGTTGTA -3' 3'- GTGTAAT <sup>S</sup> ACAACAT -5'	38 <sup>[a]</sup> 79 <sup>[b]</sup>

[a]  $T_m$  value for renaturing curve. [b]  $T_m$  value for denaturing curve.

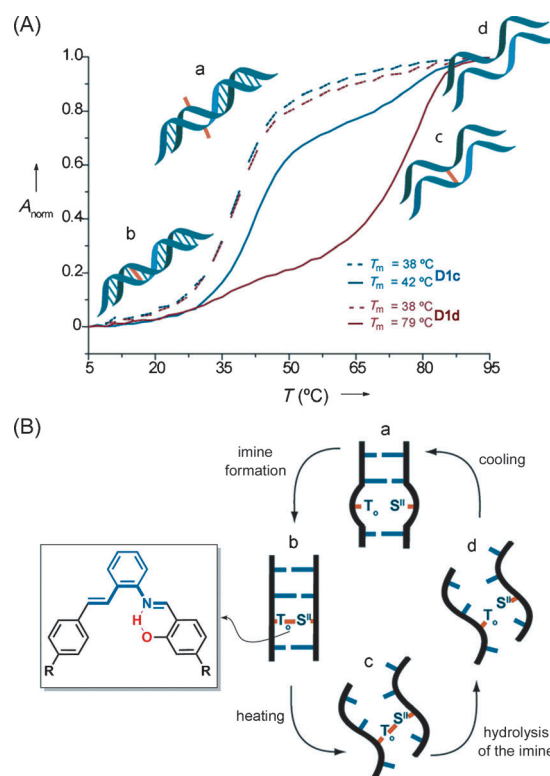


**Figure 2.** A) Melting profiles obtained from duplex **D1c**, showing the denaturing curve (blue solid line) and renaturing curve (blue dashed line), and duplex **D1d**, showing the denaturing curve (red solid line) and renaturing curve (red dashed line). Experiments were monitored at 260 nm in 150 mM NaCl, 10 mM CHES pH 9 with 2  $\mu\text{M}$  concentration for duplexes **D1a-d**. B) Model proposed for the melting and the annealing processes.

trifluoroacetyl group and all other protecting groups and afforded the oligonucleotide cleavage from the solid support.<sup>[14]</sup> We subsequently evaluated the biophysical properties of the cross-links  $\text{T}_0\text{:S}^{\text{I}}$  and  $\text{T}_0\text{:S}^{\text{II}}$ . First, the melting temperatures of all the synthesized duplexes (Table 1) were determined by UV spectroscopy. As an example, Figure 2A shows the typical melting curves measured for **D1c** and **D1d**.

Under the chosen conditions, the reference duplex **D1a**, (A:T) had a melting point of  $48^{\circ}\text{C}$ .<sup>[15]</sup> The melting temperature dropped to  $T_m = 35^{\circ}\text{C}$  when the central A:T unit was replaced by a A:C mismatch (**D1b**). The duplex with a  $\text{T}_0\text{:S}^{\text{I}}$  (**D1c**) had a  $T_m$  value of  $42^{\circ}\text{C}$ . This result shows that  $\text{T}_0\text{:S}^{\text{I}}$  lacking the phenolic OH group creates a rather destabilizing situation, with the imine linkage not established (Figure 2A). In sharp contrast, the duplex **D1d** containing the  $\text{T}_0\text{:S}^{\text{II}}$  cross-link (with the phenolic OH group) displayed a high melting point of  $79^{\circ}\text{C}$  (Figure 2A). This result confirms our hypothesis of the hydroxy group stabilizing the formed imine through an intramolecular hydrogen bond.<sup>[16]</sup>

It is interesting that, while the curves obtained from the melting and annealing of natural oligonucleotides are superimposable in typical melting experiments, substantial hysteresis was observed for the duplex **D1d** (Figure 2A). We explain this feature of  $\text{T}_0\text{:S}^{\text{II}}$  with a model that involves a slow rate of imine hydrolysis and formation (Figure 2B). Upon

heating, the canonical base pairs melt, but the duplex is still held together by the central  $T_o:S^{II}$  cross-link (c) until the imine bond is also hydrolyzed (d). During cooling, the flanking natural bases might assemble again first, while the central noncanonical cross-link represents initially a typical mismatch (a), which is slowly converted into a stabilizing imine-connected covalent linkage (b).

To gain support for the proposed mechanism, we studied the UV-melting properties on variation of the heating and cooling rates. Indeed, the size of the hysteresis effect showed a critical rate dependence.<sup>[17]</sup> When we decreased the heating/cooling steps from  $0.5^\circ\text{C min}^{-1}$  ( $\Delta T_m = 31.5$ ) to  $0.1^\circ\text{C min}^{-1}$  ( $\Delta T_m = 18.5$ ) we observed a strongly reduced hysteresis, while increased hysteresis was detected when the heating rate was increased from  $0.1^\circ\text{C min}^{-1}$  to  $1.0^\circ\text{C min}^{-1}$  ( $\Delta T_m = 39.0$ ). These results support the idea that imine formation, and hence the establishment of the covalent bond, is the rate-determining step in the assembly process of the duplex.

We next investigated whether the  $T_o:S^{II}$  cross-link can be created enzymatically. This is of interest when the construction of longer DNA strands is required. Therefore, we inserted the  $T_o$  base into a 30-mer oligonucleotide template and hybridized it to a 23-mer primer strand ending one base before the  $T_o$  unit (Figure 3A). The deoxy- $S^{II}$  triphosphate

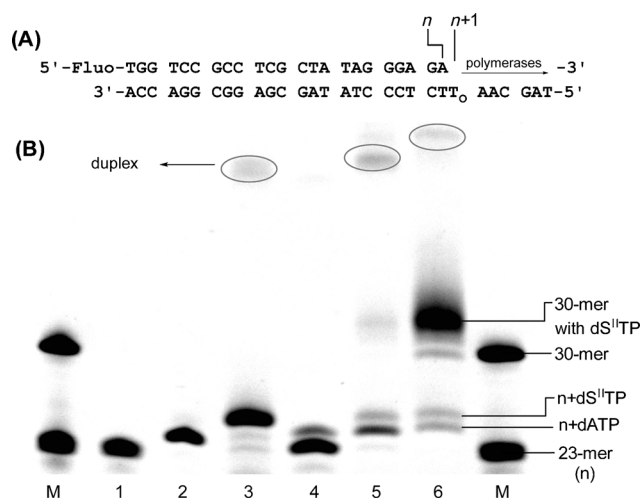


**Figure 3.** A) Sequence of the template and primer strands. The primer was labeled at the 5' end with fluorescein. B) PAGE from primer extension experiments using 1 pmol template, 200  $\mu\text{M}$  dNTPs, 400  $\mu\text{M}$   $dS^{II}TP$ , 2 U polymerase. M: marker, lane 1: negative control, lane 2: +1 positive control (24-mer); lane 3: single nucleotide insertion  $dS^{II}TP$  only (10 min, Kf,  $37^\circ\text{C}$ ); lane 4: similar to lane 3 but addition of dNTPs only; lane 5: dXTPs (6 h, Kf ( $\text{exo}^-$ )); lane 6: dXTPs two polymerases (1. Kf, then Bst Pol I; 2. 10 min,  $37^\circ\text{C}$ ; 3. 6 h,  $60^\circ\text{C}$ ). Note that a sequential addition of components is not required.

( $dS^{II}TP$ ) was synthesized (see p.13 in the Supporting Information), and various polymerases and conditions were systematically screened for their ability to create the  $T_o:S^{II}$  cross-link. Initial kinetic studies showed that the Klenow polymerase (Kf) was able to incorporate  $dS^{II}TP$  opposite  $T_o$  quantitatively in only 10 min (see Figure S6 in the Supporting Information). Notably, in comparison to the +1 positive

control, in which the  $T_o:S^{II}$  cross-link is replaced by an A:T pair, the  $dS^{II}$ -incorporated 24-mer migrates slower in the polyacrylamide gel electrophoresis (PAGE) experiments (Figure 3B, lanes 3 and 5). This is in accordance with observations already reported for the  $S^{II}$  homopair.<sup>[18]</sup> We next studied the enzymatic selectivity of the  $dS^{II}TP$  incorporation opposite the  $T_o$  base. Kf was found to provide sufficient selectivity. Only dATP was misincorporated to some extent (see Figure S7 in the Supporting Information). Although  $dS^{II}TP$  yielded the +1 elongated primer almost completely (Figure 3B, lane 3), all the dNTPs applied to the single nucleotide insertion resulted in mostly non-elongated primer (Figure 3B, lane 4).

Despite denaturing conditions during PAGE (7M urea) and extensive heating of the samples before loading ( $95^\circ\text{C}$ , 10 min), we detected bands in the gel that originate from the duplex (Figure 3B). The cross-link clearly stabilizes the double helix to an extent that some of the duplexes do not melt, in agreement with the intended stabilizing effect.

We next studied the possibility of creating fully elongated primers. We first experimented with all five dXTPs (four dNTPs and  $dS^{II}TP$ ) and the Kf( $\text{exo}^-$ ) polymerase. In this case, a very faint band of the fully elongated 30-mer product was detected in addition to a prominent 24-mer and a 25-mer elongated primer (Figure 3B, lane 5). Although Kf( $\text{exo}^-$ ) is clearly able to provide some full extension, the best results were finally obtained with a combination of the polymerases Kf and Bst Pol I in the presence of all the dXTPs (Figure 3B, lane 6).<sup>[19]</sup> In this case, the fully extended primer is the main product.

Again, some of the duplexes even survive the denaturing gel electrophoresis conditions. When we next performed primer extension studies with the  $dT_oTP$  (for the synthesis see p. 14 in the Supporting Information) using a  $S^{II}$  base in the template, we found that incorporation of  $dT_o$  opposite the templating  $S^{II}$  is also possible using the polymerases Kf, Bst Pol I, and others (see Figure S9 in the Supporting Information). Quantitative single nucleotide insertion was observed for Kf in 20 min (see Figure S10 in the Supporting Information). The selectivity of the enzymatic  $dT_oTP$  incorporation resembles the results of  $dS^{II}TP$  incorporation opposite  $T_o$ . Again, dA misinsertion was obtained to some extent, while only the artificial  $dT_oTP$  quantitatively yields the +1 elongated primer (see Figure S11 in the Supporting Information). In this case, full extension proved to be more difficult and only small amounts of the full length product are formed (see Figure S12 in the Supporting Information).

To learn about the bioisoteric nature of the  $T_o:S^{II}$  cross-link, we cocrystallized a DNA double strand containing the cross-link at position  $n-5$  in complex with Bst Pol I (Figure 4A, PDB code 4UQG). In this experiment the cross-link is outside the active site of the polymerase, which served just a crystallization scaffold. The structure shows that the  $T_o:S^{II}$  bases face each other and that they are covalently linked through the expected imine interaction.

An overlay with a structure of a canonical dG:dC base pair at this position shows that the  $T_o:S^{II}$  cross-link provokes only small structural perturbations in the duplex (Figure 4B). The distance of 10.8 Å between the C1' atoms in the

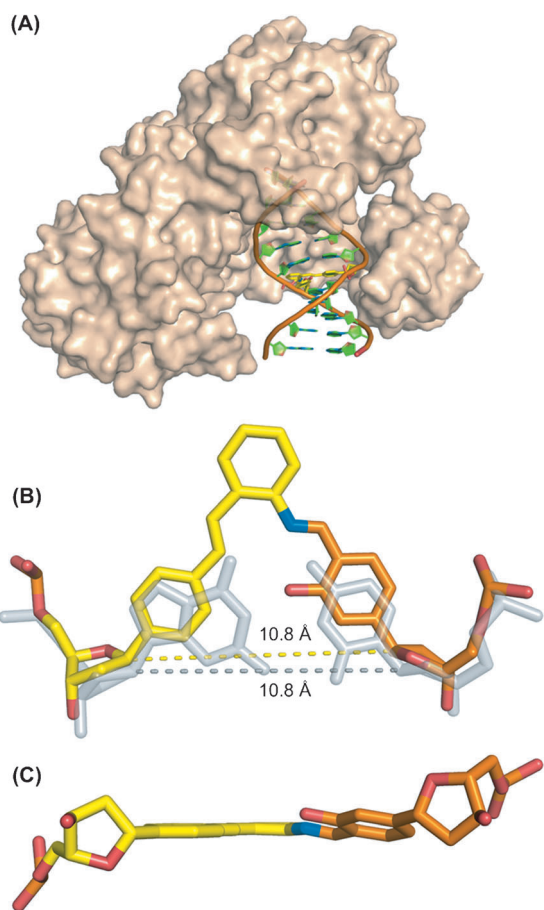


**Figure 4.** A) Crystal structure of Bst Pol I in complex with a  $T_0:S^{II}$  cross-link-containing DNA. B) The  $T_0:S^{II}$  cross-link overlaid with a canonical dG:dC base pair. The C1'-C1' distance of 10.8 Å for the unnatural cross-link is identical with the distance observed for the canonical base pair. C) Rear view of the  $T_0:S^{II}$  cross-link, showing a twist out of the plane.  $T_0$  is depicted in yellow,  $S^{II}$  in orange. For the electron density of B) and C) see Figure S14.

deoxyribose moieties of the artificial cross-link is practically identical to that in the natural base pair. In contrast, the previously reported metal- and ethylenediamine-mediated  $S^{II}$  homobase pair has a distance of 11.4 Å (see Figure S15 in the Supporting Information). The improved fit of the  $T_0:S^{II}$  cross-link is achieved because  $T_0$  adopts a conformation, which we did not expect, with the stilbene double bond rotated away from the counterbase. It could be that the need to populate this rotameric conformation is the reason for the sluggish full elongation after  $dT_0TP$  incorporation opposite a  $S^{II}$  template.

The  $T_0:S^{II}$  cross-link is not perfectly planar, with  $S^{II}$  slightly twisted from the  $T_0$  plane (Figure 4C). The oxygen atom from the  $S^{II}$  base and the imine bond are in the same plane, similar to a bicyclic system, trying to avoid steric clash with the alkene.

In conclusion, we report a new  $T_0:S^{II}$  cross-linking unit that allows the formation of selective, reversible, and most important, highly thermostable DNA interstrand cross-links, based on the concept of reversible imine chemistry. Primer extensions showed that enzymatic incorporation of the cross-link is also possible, particularly with the  $T_0$  base in the

template strand. The crystal structure reveals that  $T_0:S^{II}$  mimics the shape of the canonical base pairs. We believe that the “post-it”-type cross-link will be helpful in the assembly of stabilized DNA nanostructures.

Received: August 1, 2014

Published online: ■ ■ ■ ■ ■, ■ ■ ■ ■ ■

**Keywords:** DNA · DNA cross-linking · DNA nanostructures · imines · reversible bonding

- [1] a) F. Zhang, J. Nangreave, Y. Liu, H. Yan, *J. Am. Chem. Soc.* **2014**, *136*, 11198–11211; b) J.-L. H. A. Duprey, Y. Takezawa, M. Shionoya, *Angew. Chem. Int. Ed.* **2013**, *52*, 1212–1216; *Angew. Chem.* **2013**, *125*, 1250–1254; c) B. Saccà, C. M. Niemeyer, *Angew. Chem. Int. Ed.* **2012**, *51*, 58–66; *Angew. Chem.* **2012**, *124*, 60–69; d) E. S. Andersen, M. Dong, M. M. Nielsen, K. Jahn, R. Subramani, W. Mamdouh, M. M. Golas, B. Sander, H. Stark, C. L. P. Oliveira, J. S. Pedersen, V. Birkedal, F. Besenbacher, K. V. Gothelf, J. Kjems, *Nature* **2009**, *459*, 73–76; e) S. M. Douglas, H. Dietz, T. Liedl, B. Högberg, F. Graf, W. M. Shih, *Nature* **2009**, *459*, 414–418; f) P. W. K. Rothmund, *Nature* **2006**, *440*, 297–302; g) W. M. Shih, J. D. Quispe, G. F. Joyce, *Nature* **2004**, *427*, 618–621; h) N. C. Seeman, *Nature* **2003**, *421*, 427; i) J. Chen, N. C. Seeman, *Nature* **1991**, *350*, 631–633.
- [2] a) T. Tørring, N. V. Voigt, J. Nangreave, H. Yan, K. V. Gothelf, *Chem. Soc. Rev.* **2011**, *40*, 5636–5646; b) A. V. Pinheiro, D. Han, W. M. Shih, H. Yan, *Nat. Nanotechnol.* **2011**, *6*, 763–772; c) F. A. Aldaye, A. L. Palmer, H. F. Sleiman, *Science* **2008**, *321*, 1795–1799; d) K. V. Gothelf, T. H. LaBean, *Org. Biomol. Chem.* **2005**, *3*, 4023–4037; e) J. Wengel, *Org. Biomol. Chem.* **2004**, *2*, 277–280.
- [3] a) Z.-G. Wang, B. Ding, *Adv. Mater.* **2013**, *25*, 3905–3914; b) Y. Zhang, F. Lu, K. G. Yager, D. van der Lelie, O. Gang, *Nat. Nanotechnol.* **2013**, *8*, 865–872; c) M. Endo, Y. Yang, H. Sugiyama, *Biomater. Sci.* **2013**, *1*, 347–360; d) O. I. Wilner, I. Willner, *Chem. Rev.* **2012**, *112*, 2528–2556; e) Y. Krishnan, F. C. Simmel, *Angew. Chem. Int. Ed.* **2011**, *50*, 3124–3156; *Angew. Chem.* **2011**, *123*, 3180–3215.
- [4] a) M. R. Hartman, D. Yang, T. N. N. Tran, K. Lee, J. S. Kahn, P. Kiatwuthinon, K. G. Yancey, O. Trotsenko, S. Minko, D. Luo, *Angew. Chem. Int. Ed.* **2013**, *52*, 8699–8702; *Angew. Chem.* **2013**, *125*, 8861–8864; b) S. H. Park, P. Yin, Y. Liu, J. H. Reif, T. H. LaBean, H. Yan, *Nano Lett.* **2005**, *5*, 729–733.
- [5] A. Banerjee, D. Bhatia, A. Saminathan, S. Chakraborty, S. Kar, Y. Krishnan, *Angew. Chem. Int. Ed.* **2013**, *52*, 6854–6857; *Angew. Chem.* **2013**, *125*, 6992–6995.
- [6] a) M. Ye, J. Guillaume, Y. Liu, R. Sha, R. Wang, N. C. Seeman, J. W. Canary, *Chem. Sci.* **2013**, *4*, 1319–1329; b) M. Endo, T. Majima, *Angew. Chem. Int. Ed.* **2003**, *42*, 5744–5747; *Angew. Chem.* **2003**, *115*, 5922–5925; c) M. Endo, T. Majima, *J. Am. Chem. Soc.* **2003**, *125*, 13654–13655; d) S. Alefeldler, S. T. Sigurdsson, *Bioorg. Med. Chem.* **2000**, *8*, 269–273; e) G. D. Glick, *Biopolymers* **1998**, *48*, 83–96; f) S. A. Wolfe, A. E. Ferentz, V. Grantcharova, M. E. A. Churchill, G. L. Verdine, *Chem. Biol.* **1995**, *2*, 213–221; g) N. C. Chaudhuri, E. T. Kool, *J. Am. Chem. Soc.* **1995**, *117*, 10434–10442.
- [7] a) J. T. Millard, S. Raucher, P. B. Hopkins, *J. Am. Chem. Soc.* **1990**, *112*, 2459–2460; b) S. E. Sherman, D. Gibson, A. H. J. Wang, S. J. Lippard, *Science* **1985**, *230*, 412–417.
- [8] A. Rajendran, M. Endo, Y. Katsuda, K. Hidaka, H. Sugiyama, *J. Am. Chem. Soc.* **2011**, *133*, 14488–14491.
- [9] a) B. A. Yard, L. G. Carter, K. A. Johnson, I. M. Overton, M. Dorward, H. Liu, S. A. McMahon, M. Oke, D. Puech, G. J. Barton, J. H. Naismith, D. J. Campopiano, *J. Mol. Biol.* **2007**,

- 370, 870–886; b) A. E. Beattie, D. J. Clarke, J. M. Wadsworth, J. Lowther, H.-L. Sin, D. J. Campopiano, *Chem. Commun.* **2013**, 49, 7058–7060.
- [10] N. E. Price, K. M. Johnson, J. Wang, M. I. Fekry, Y. Wang, K. S. Gates, *J. Am. Chem. Soc.* **2014**, 136, 3483–3490.
- [11] N. Joubert, M. Urban, R. Pohl, M. Hocek, *Synthesis* **2008**, 1918–1932.
- [12] G. H. Clever, K. Polborn, T. Carell, *Angew. Chem. Int. Ed.* **2005**, 44, 7204–7208; *Angew. Chem.* **2005**, 117, 7370–7374.
- [13] In that case, the amino group underwent cleavage of the trifluoroacetyl group and further acetyl protection. The acetyl group could not be removed during final deprotection.
- [14] Some other protecting groups were tested before, such as the benzoyl and the acetyl group. Unfortunately, the deprotection strategies always failed.
- [15] Buffer CHES pH 9 was used according to previous studies in the group (see Refs. [12] and [18]). Nevertheless, pH 7 and pH 8 conditions have also been studied (with different buffers). The results are similar to the experiments performed at pH 9. The denaturing/renaturing behavior of duplex **D1d** under variation of the pH conditions is presented in Figures S2 and S3 as well as Table S4 in the Supporting Information.
- [16] Melting point experiments to study the selectivity of the  $T_m$  towards the canonical bases have been performed. The results are shown in Figure S1 in the Supporting information.
- [17] The feature of hysteresis as well as the same tendency of rate dependence are observed under different pH conditions. However, at pH 7 and pH 8 the hysteresis is always smaller (independently of the buffer employed). The maximum value is achieved at pH 9. The results are shown in Figures S2 and S3 in the Supporting Information.
- [18] C. Kaul, M. Müller, M. Wagner, S. Schneider, T. Carell, *Nat. Chem.* **2011**, 3, 794–800.
- [19] E. L. Tae, Y. Wu, G. Xia, P. G. Schultz, F. E. Romesberg, *J. Am. Chem. Soc.* **2001**, 123, 7439–7440.
-

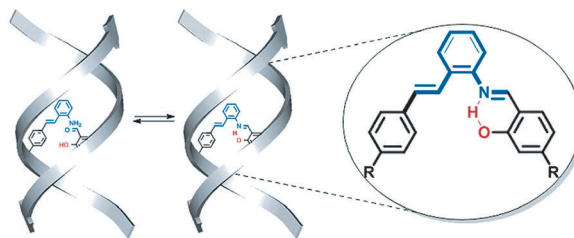
## Communications



### Covalent Reversible Cross-Linking

M. Tomás-Gamasa, S. Serdjukow, M. Su,  
M. Müller, T. Carell\* ——— ■■■■—■■■■

“Post-It” Type Connected DNA Created  
with a Reversible Covalent Cross-Link



**Reversible bond formation** was used as a design principle to create a “post-it”-type cross-linking unit. The aldehyde–

amine DNA cross-link endows DNA duplexes with a reversible but unusual high stability.